JACS
JOURNAL OF THE AMERICAN CHEMICAL SOCIETY
pubs.acs.org/JACS
Communication

Mixed Ionic and Electronic Conductivity in a Tetrathiafulvalene-Phosphonate Metal−Organic Framework

Catarina Ribeiro, Bowen Tan, Flávio Figueira, Ricardo F. Mendes, Joaquín Calbo, Gonçalo Valente, Paula Escamilla, Filipe A. Almeida Paz, João Rocha, Mircea Dincă, and Manuel Souto*

Cite This: J. Am. Chem. Soc. 2025, 147, 63−68
Read Online
ACCESS | Metrics & More | Article Recommendations | Supporting Information

ABSTRACT: Mixed ionic-electronic conductors have great potential as materials for energy storage applications. However, despite their promising properties, only a handful of metal−organic frameworks (MOFs) provide efficient pathways for both ion and electron transport. This work reports a proton−electron dual-conductive MOF based on tetrathiafulvalene(TTF)-phosphonate linkers and lanthanum ions. The formation of regular, partially oxidized TTF stacks with short S···S interactions facilitates electron transport via a hopping mechanism, reporting a room-temperature conductivity of 7.2×10^{-6} S cm^{-1}. Additionally, the material exhibits a proton conductivity of 4.9×10^{-5} S cm^{-1} at 95% relative humidity conditions due to the presence of free −POH groups, enabling efficient proton transport pathways. These results demonstrate the potential of integrating electroactive building blocks along with phosphonate groups toward the development of mixed ionic-electronic conductors.

Downloaded via MASSACHUSETTS INST OF TECHNOLOGY on February 5, 2025 at 16:45:31 (UTC).
See https://pubs.acs.org/sharingguidelines for options on how to legitimately share published articles.

The design of mixed ionic-electronic conductors has attracted much attention for applications in bioelectronics, neuromorphics, and energy storage, because of their ability to facilitate efficient mass and charge transport.[1−4] This behavior has been observed in materials such as conjugated polymers and other organic compounds.[2,5] Metal−organic frameworks (MOFs) hold great promise for conducting both ions and electrons as their structure and electronic properties can be adjusted by the judicious selection of the building blocks.[6−8] Despite this potential, MOFs exhibiting mixed conductivity remain scarce.[8] Recently, some 2D MOFs have been reported to exhibit dual electron−proton conductivity, sometimes requiring postsynthetic modifications.[9−11] Therefore, new design strategies are needed to promote efficient electron and ion transport within a single framework material.

One strategy for designing electrically conductive MOFs involves incorporating electroactive organic moieties that may promote $\pi-\pi$ interactions, facilitating *through-space* charge transport pathways.[6,7,12] For example, some tetrathiafulvalene (TTF)-based linkers have been used to construct conductive MOFs by forming $\pi-\pi$ stacking columns with relatively short S···S interactions between the electroactive units.[13−19] The reported MOFs are based on TTF linkers typically functionalized with carboxylate or pyridyl groups.[20] More recently, coupled ion/pseudocapacitive conduction has been observed in a MOF based on a TTF-octacarboxylic acid ligand.[21] Although this MOF exhibits high proton conductivity at high relative humidity (RH), it lacks clear electron transport pathways because of the large distance between the TTF moieties, ruling out a mixed ionic/electronic conduction mechanism.[21]

An effective approach to achieve high proton conductivity in MOFs is to incorporate free phosphonate or sulfonate groups, which can increase proton concentration and mobility within the framework.[22] In addition, these free protons can be exchanged with ions (e.g., Li^+, Na^+, K^+) via acid−base reactions, a feature highly relevant for energy storage applications.[8,23,24] In this context, the use of phosphonate linkers has led to some of the highest reported proton conductivities in MOFs.[24−28] Furthermore, some phosphonate-based MOFs have shown high electrical conductivity,[29,30] although their transport mechanism has yet to be investigated.

Herein, we report a mixed ion-electron conducting MOF (**TTFTP-La**) constructed from a TTF-phosphonate-based linker and lanthanum ions. The TTF moieties are arranged in regular stacks with short intermolecular S···S interactions, ultimately facilitating an electron transport pathway. Electrical measurements using four-contact probe pressed pellet devices revealed room-temperature conductivity of 7.2×10^{-6} S cm^{-1}, and theoretical calculations further support a hopping transport mechanism involving partially oxidized TTF moieties. The proton conductivity of **TTFTP-La** was found to be 4.9×10^{-5} S cm^{-1} at 95% RH, driven by the presence of a large number of noncoordinated −POH groups within the framework that provide efficient ion transport pathways.

The TTF-tetraphenylphosphonic acid (H_8TTFTP) ligand (Scheme 1) was synthesized in two steps. First, the TTF diethyl phenylphosphonate derivative was obtained via a palladium-catalyzed C−H arylation[31,32] of TTF with diethyl (4-bromophenyl)phosphonate. This was followed by transesterification with bromotrimethylsilane[33] and subsequent hydrolysis to yield the TTF phosphonic acid derivative,

Received: October 2, 2024
Revised: December 12, 2024
Accepted: December 15, 2024
Published: December 19, 2024

ACS Publications
© 2024 American Chemical Society

https://doi.org/10.1021/jacs.4c13792
J. Am. Chem. Soc. 2025, 147, 63−68

Scheme 1. Molecular Structure of the H_8TTFTP Ligand

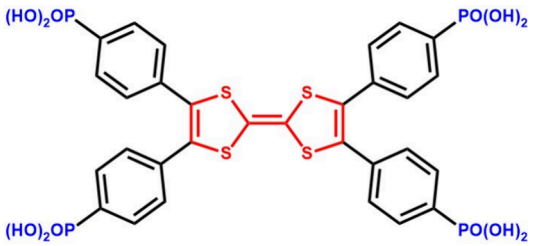

which was fully characterized (Schemes S1−S2 and Figures S1−S11).

Single crystals of **TTFTP-La** were obtained by reacting H_8TTFTP, La_2O_3 and HCl in a mixture of water and ethanol (1:1) at 160 °C for 48 h (Scheme S3). The resulting bulk material was thoroughly washed with solvents to remove any remaining precursors. The structure of the material was unveiled by single-crystal X-ray diffraction. **TTFTP-La** MOF crystallizes in the centrosymmetric triclinic space group $P\bar{1}$ (see Table S1). The asymmetric unit consists of six crystallographically independent linkers and four lanthanum metal centers, with the overall formula being $[La_4(H_{8-x}TTF)_6(H_2O)_3]\cdot 1.7EtOH\cdot 13.75H_2O$ (x = 0−3). Variations in the protonation levels of the organic linkers dictate the overall connectivity of the MOF. Of the 24 independent phosphonate groups, only three bind to the lanthanum centers via μ_2-*O,O* coordination mode, while the others connect via simpler k^1-*O* or k^2-*O* modes. The connection of the La-phosphonate chains with the TTF linkers forms a dense structure (Figure 1a), although microporous cavities within the framework create a calculated free volume of ∼11% of the unit cell volume (Figure S12).

The TTF moieties are arranged in one-dimensional stacked columns along the *b*-axis with relatively short S···S distances (∼3.6 Å) between adjacent TTF units (Figure 1b). These distances are shorter than those observed in other TTF-based MOFs,[13,15] which may favor a better overlap between the sulfur $3p_z$ orbitals, thereby facilitating a more efficient electron transport. It is important to note that lanthanides also play an important role in determining the TTF packing motif and intermolecular S···S distances due to their highly flexible coordination environment. Thus, the combination of TTF linkers with distinct lanthanides can lead to different structures with modulated conductivities.[15,16] Notably, the TTF linkers exhibit two stacking patterns: some TTF linkers are arranged in a parallel manner, while others are stacked in a rotated arrangement along the *b*-axis (Figures 1b, S13 and S14). Despite the significant steric hindrance caused by the numerous phenylphosphonic groups, this compact packing is made possible thanks to the flexibility of the TTF moieties. Indeed, only two of the six TTF linkers adopted a planar conformation (typical of TTF radical cation species), while the rest exhibited a boat-like conformation (Figure S15). An analysis of the intramolecular distances and dihedral angles of the TTF linkers suggests that there is a mixture of neutral and radical cation TTF species. The calculated charges for TTF moieties, estimated by considering the bond length (C=C/C−S) ratio (Table S2),[15,34] range from +0.1 to +0.6. This partial oxidation of the TTF linkers was further supported by electron paramagnetic resonance (EPR) measurements, showing a signal at g = 2.006 characteristic of organic radical species, which was more intense than that observed for the H_8TTFTP ligand (Figure S16). Raman spectroscopy further confirmed the presence of TTF moieties with varying degrees of charge, ranging from neutral to radical cation species, within the framework (Figure S17).[35] Additionally, the proximity of the free −POH groups (Figure 1c) may facilitate proton transport through a hydrogen-bonding network.

The material was further characterized to investigate its physicochemical properties. The Fourier transformed infrared (FTIR) spectrum of the **TTFTP-La** shows a small shift in the phosphonate bands compared to that of the ligand that can be attributed to the coordination of the phosphonate groups to lanthanum (Figure S18).[28] In addition, the broad bands around 3000−3300 cm^{-1}, attributed to OH stretching bands, further support the presence of free −POH groups.[36−38] The homogeneous distribution of all elements present in the material was confirmed by energy-dispersive X-ray spectroscopy (Figure S19). Thermogravimetric analysis of the activated **TTFTP-La** shows a mass loss of ∼6% between 25 and 180 °C (Figure S20), corresponding to the release of water and ethanol molecules. The material is stable up to 300 °C, consistent with the linker degradation observed in other TTF-based MOFs,[39] and further confirmed by powder X-ray diffraction (PXRD) at high temperatures (Figure S21). In

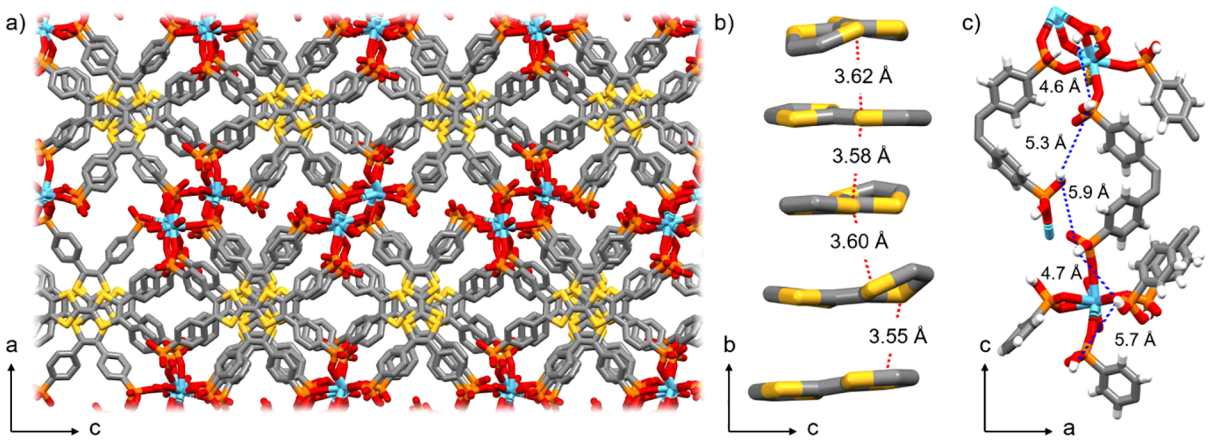

Figure 1. (a) View of the crystal structure of **TTFTP-La** along the *b*-axis. (b) Lateral view of a TTF stack, highlighting the shortest intermolecular S···S distances. (c) Arrangement of La^{3+} ions and phosphonate groups, displaying the distances between adjacent free −POH groups. Color code: C (gray), O (red), La (blue), S (yellow), P (orange), H (white).

https://doi.org/10.1021/jacs.4c13792
J. Am. Chem. Soc. 2025, 147, 63−68

addition, the material shows good chemical stability in aqueous solution and different organic solvents (Figure S22). Gas sorption measurements were performed on the activated **TTFTP-La** MOF (heated to 150 °C for 12 h under vacuum). The CO_2 adsorption isotherm at 273 K shows an uptake of 80 $cm^3\ g^{-1}$ at 1 bar, and the pore size distribution analysis revealed a pore size of 4.1 Å (Figure S23). In contrast, the N_2 adsorption−desorption isotherm at 77 K reveals a minimal uptake of N_2, consistent with other microporous TTF-based MOFs.[15,40] This selective adsorption of CO_2 over N_2 is attributed to the high quadrupole moment of CO_2 molecules that interact favorably with the large π-electron cloud of the electroactive linkers.[41] The redox activity of **TTFTP-La** was investigated by solid-state cyclic voltammetry (Figure S24), showing two reversible redox processes attributed to the subsequent oxidation of the TTF moieties to the radical cation and dication species.[7]

Encouraged by the partial oxidation and the short distance between adjacent TTF moieties, electrical measurements were carried out on pressed polycrystalline pellets using four-contact probe measurements (see Supporting Information (SI) for measurement details). **TTFTP-La** MOF exhibits a conductivity of 7.2×10^{-6} S cm^{-1} at 296 K at ambient atmosphere (60% RH), situating it in the upper echelon for TTF-based MOFs (Table S3).[6] The room-temperature (300 K) conductivity measured under high vacuum was found to be 2.9×10^{-6} S cm^{-1}, confirming the presence of the electronic component of the mixed conductivity. Variable-temperature (VT) conductivity measurements reveal that this material shows thermally activated transport (Figures 2 and S25), which is typical for

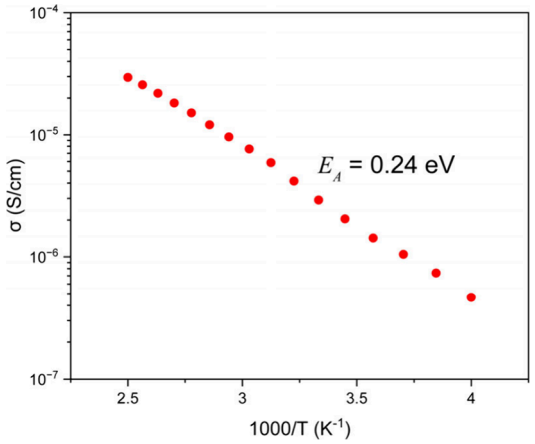

Figure 2. Variable temperature conductivity of **TTFTP-La** between 250 and 400 K.

semiconductors. Fitting the VT conductivity data to an Arrhenius model gives a linear relationship with $1/T$ between 400 and 250 K, yielding an E_A of 0.24 eV. The activation energies correspond to the hopping energy barriers based on the nearest neighbor hopping mechanism. An optical bandgap (E_g) of 1.58 eV was obtained by linearly fitting the absorption onsets in the Tauc plots of the Kubelka−Munk-transformed data (Figure S26), which is in full agreement with theoretical calculations (see below).

To gain further insight into the charge transport mechanism, theoretical calculations were performed using density functional theory (DFT) within periodic boundary conditions to characterize the electronic properties of the TTF-based MOF (see SI for computational details). Hybrid DFT calculations (HSE06 level) show that the electronic structure of **TTFTP-La** is characterized by flat bands along the main reciprocal directions, including the $\pi-\pi$ TTF pathway (Y−Γ) (Figure 3a). This result indicates that charge transport between

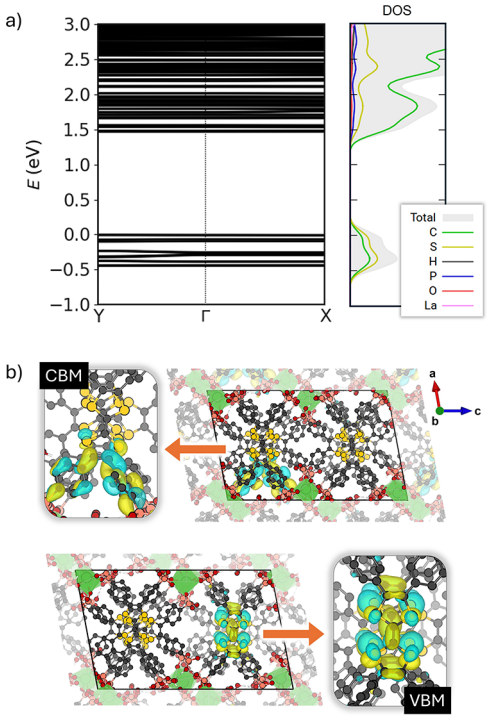

Figure 3. (a) Band structure and species-projected density of states (DOS) for **TTFTP-La** MOF, calculated at the DFT-HSE06 level of theory. The Fermi level is aligned with the valence-band maximum. (b) Frontier crystal orbitals corresponding to the valence-band maximum (VBM) and conduction-band minimum (CBM) for the MOF, calculated at the DFT-HSE06 level of theory with an isovalue of 0.05.

neighboring TTF units occurs via a hopping mechanism. The species-projected density of states suggests that both the valence-band maximum (VBM) and the conduction-band minimum (CBM) are located on the TTFTP ligand. Visualization of the frontier crystal orbitals confirms the localization of the VBM in the TTF moiety, whereas the CBM is distributed over the phenylphosphonate group (Figure 3b). The calculated band gap for the MOF is 1.47 eV, in good accord with the experimental data, and slightly smaller than that predicted at the same level of theory for the related X_2(TTFTB) family (1.75 eV).[13]

Temperature-dependent proton conductivity measurements on **TTFTP-La** were performed at different RH values (see SI for measurement details) (Figures 4 and S27−29). The material exhibits a conductivity of 3.1×10^{-6} S cm^{-1} at 35% RH and room temperature, increasing to 4.9×10^{-5} S cm^{-1} at 95% RH and 333 K. The Arrhenius plot demonstrates that proton conductivity rises with increasing temperature across all humidity conditions. The calculated activation energies were 0.12, 0.15, and 0.34 eV for 35%, 65%, and 95% RH, respectively. This relatively low activation energy suggests the Grotthuss mechanism (E_A < 0.4 eV),[42] where the protons diffuse through hydrogen-bonding network between non-coordinated −POH functional groups within the framework.

https://doi.org/10.1021/jacs.4c13792
J. Am. Chem. Soc. 2025, 147, 63−68

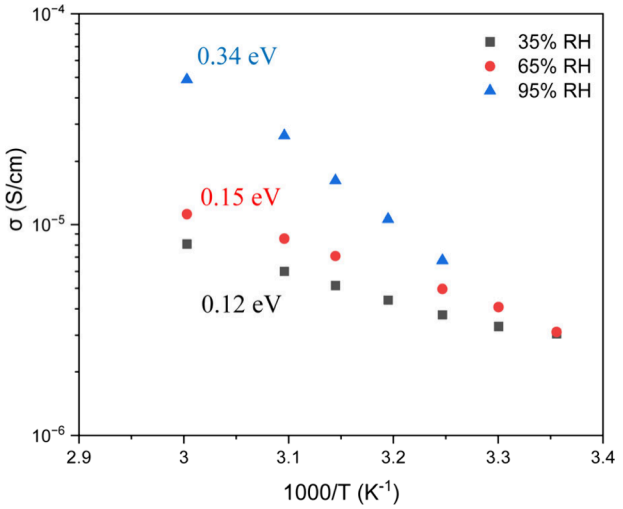

Figure 4. Arrhenius plot showing the proton conductivity of the **TTFTP-La** MOF measured across a range of temperatures and relative humidity (RH) levels.

The proton conductivity values are similar to those of other phosphonate-based MOFs,[24] and lower than those of another TTF-based MOF.[21] Current research focuses on combining the TTFTP linker with other metals and conducting postsynthetic proton/cation exchange to incorporate alkali cations into the framework, aiming to investigate the influence on ionic and electronic conductivity.[23,24,43]

In conclusion, we have shown that the construction of MOFs based on properly stacked electroactive linkers functionalized with phosphonate groups can create efficient electron and proton transport pathways through the framework. The semiconducting behavior of **TTFTP-La** was attributed to the presence of short intermolecular S···S interactions between adjacent partially oxidized TTF moieties, enabling a hopping transport mechanism. Additionally, the proton conductivity increased with the relative humidity, as the hydrogen-bonding network formed between the numerous noncoordinated −POH groups enables proton diffusion. These findings provide a new molecular design approach for the development of MOF-based mixed ionic-electronic conductors for energy storage, among other applications.

■ ASSOCIATED CONTENT

Supporting Information

The Supporting Information is available free of charge at https://pubs.acs.org/doi/10.1021/jacs.4c13792.

General methods and materials, synthesis and characterization of H_8TTFTP and TTFTP-La MOF, electrical and proton conductivity measurements, theoretical calculations. (PDF)

Accession Codes

Deposition Number 2383921 contains the supplementary crystallographic data for this paper. These data can be obtained free of charge via the joint Cambridge Crystallographic Data Centre (CCDC) and Fachinformationszentrum Karlsruhe Access Structures service.

■ AUTHOR INFORMATION

Corresponding Author

Manuel Souto − *CIQUS, Centro Singular de Investigación en Química Bioloxica e Materiais Moleculares, Departamento de Química-Física, Universidade de Santiago de Compostela, 15782 Santiago de Compostela, Spain; Department of Chemistry, CICECO-Aveiro Institute of Materials, University of Aveiro, 3810-393 Aveiro, Portugal; Oportunius, Galician Innovation Agency (GAIN), 15702 Santiago de Compostela, Spain;* orcid.org/0000-0003-3491-6984; Email: manuel.souto.salom@usc.es

Authors

Catarina Ribeiro − *Department of Chemistry, CICECO-Aveiro Institute of Materials, University of Aveiro, 3810-393 Aveiro, Portugal*

Bowen Tan − *Department of Chemistry, Massachusetts Institute of Technology, Cambridge, Massachusetts 02139, United States;* orcid.org/0000-0002-5166-1541

Flávio Figueira − *Department of Chemistry, CICECO-Aveiro Institute of Materials, University of Aveiro, 3810-393 Aveiro, Portugal;* orcid.org/0000-0002-3685-9736

Ricardo F. Mendes − *Department of Chemistry, CICECO-Aveiro Institute of Materials, University of Aveiro, 3810-393 Aveiro, Portugal;* orcid.org/0000-0001-8242-324X

Joaquín Calbo − *Instituto de Ciencia Molecular (ICMol), Universidad de Valencia, 46980 Paterna, Spain;* orcid.org/0000-0003-4729-0757

Gonçalo Valente − *Department of Chemistry, CICECO-Aveiro Institute of Materials, University of Aveiro, 3810-393 Aveiro, Portugal*

Paula Escamilla − *CIQUS, Centro Singular de Investigación en Química Bioloxica e Materiais Moleculares, Departamento de Química-Física, Universidade de Santiago de Compostela, 15782 Santiago de Compostela, Spain;* orcid.org/0000-0002-6419-8891

Filipe A. Almeida Paz − *Department of Chemistry, CICECO-Aveiro Institute of Materials, University of Aveiro, 3810-393 Aveiro, Portugal;* orcid.org/0000-0003-2051-5645

João Rocha − *Department of Chemistry, CICECO-Aveiro Institute of Materials, University of Aveiro, 3810-393 Aveiro, Portugal;* orcid.org/0000-0002-0417-9402

Mircea Dincă − *Department of Chemistry, Massachusetts Institute of Technology, Cambridge, Massachusetts 02139, United States;* orcid.org/0000-0002-1262-1264

Complete contact information is available at: https://pubs.acs.org/10.1021/jacs.4c13792

Notes

The authors declare no competing financial interest.

■ ACKNOWLEDGMENTS

This work has received funding from the European Research Council (ERC) under the European Union's Horizon Europe Framework Programme (ERC-2021-Starting Grant, grant agreement no. 101039748-ELECTROCOFS), from the FCT/MEC (CICECO-Aveiro Institute of Materials, UIDB/50011/2020, UIDP/50011/2020, LA/P/0006/2020), FCT (PTDC/QUI-ELT/2593/2021) and from the PRR—Plano de Recuperação e Resiliência (NextGenerationEU funds) through the scope of the Agenda for Business Innovation "New Generation Storage" (project no. 58 with the application

https://doi.org/10.1021/jacs.4c13792
J. Am. Chem. Soc. 2025, 147, 63−68

C644936001−00000045). This work has also received financial support from the Xunta de Galicia (Centro singular de investigación de Galicia accreditation 2023−2027, ED431G 2023/03) and the Oportunius program (Gain). R.F.M. thanks the FCT for a Junior Research Position (10.54499/CEECIND/00553/2017/CP1459/CT0034). The research contract of FF (REF-168-89-ARH/2018) is funded by national funds (OE), through FCT, in the scope of the framework contract foreseen in Nos. 4, 5, and 6 of article 23 of the Decree-Law 57/2016, of August 29, changed by Law 57/2017, of July 19. G.V. is grateful to FCT for his PhD grant (2020.08520.BD). J.C. acknowledges the Ministry of Spain: projects PID2020-119748GA-I00 funded by MCIN/AEI/10.13039/501100011033 and TED2021-131255B-C44 funded by MCIN/AEI/10.13039/501100011033 and by European Union NextGenerationEU/PRTR. Part of the data used in the proposal was collected at the ESRF in the experiment session CH-6693 on beamline BM01 (DOI: 10.15151/ESRF-ES-1465093925). Work in the Dincă lab (B.T. and M.D.) was supported by the National Science Foundation (DMR2105495).

■ ABBREVIATIONS

MOF, Metal−Organic Framework; TTF, tetrathiafulvalene; RH, relative humidity; DOS, density of states; VBM, valence-band maximum; CBM, conduction-band minimum

■ REFERENCES

(1) Chen, C.-C.; Fu, L.; Maier, J. Synergistic, Ultrafast Mass Storage and Removal in Artificial Mixed Conductors. *Nature* **2016**, *536*, 159−164.
(2) Paulsen, B. D.; Tybrandt, K.; Stavrinidou, E.; Rivnay, J. Organic Mixed Ionic−Electronic Conductors. *Nat. Mater.* **2020**, *19*, 13−26.
(3) Hatakeyama, K.; Tateishi, H.; Taniguchi, T.; Koinuma, M.; Kida, T.; Hayami, S.; Yokoi, H.; Matsumoto, Y. Tunable Graphene Oxide Proton/Electron Mixed Conductor That Functions at Room Temperature. *Chem. Mater.* **2014**, *26*, 5598−5604.
(4) Li, J.; Wang, C.; Su, J.; Liu, Z.; Fan, H.; Wang, C.; Li, Y.; He, Y.; Chen, N.; Cao, J.; Chen, X. Observing Proton−Electron Mixed Conductivity in Graphdiyne. *Adv. Mater.* **2024**, *36*, 2400950.
(5) Kim, H.; Won, Y.; Song, H. W.; Kwon, Y.; Jun, M.; Oh, J. H. Organic Mixed Ionic−Electronic Conductors for Bioelectronic Sensors: Materials and Operation Mechanisms. *Adv. Sci.* **2024**, *11*, 2306191.
(6) Xie, L. S.; Skorupskii, G.; Dincă, M. Electrically Conductive Metal−Organic Frameworks. *Chem. Rev.* **2020**, *120*, 8536−8580.
(7) Souto, M.; Strutyński, K.; Melle-Franco, M.; Rocha, J. Electroactive Organic Building Blocks for the Chemical Design of Functional Porous Frameworks (MOFs and COFs) in Electronics. *Chem.—Eur. J.* **2020**, *26*, 10912−10935.
(8) Kharod, R. A.; Andrews, J. L.; Dincă, M. Teaching Metal-Organic Frameworks to Conduct: Ion and Electron Transport in Metal-Organic Frameworks. *Annu. Rev. Mater. Res.* **2022**, *52*, 103−128.
(9) Choi, J. Y.; Stodolka, M.; Kim, N.; Pham, H. T. B.; Check, B.; Park, J. 2D Conjugated Metal-Organic Framework as a Proton-Electron Dual Conductor. *Chem.* **2023**, *9*, 143−153.
(10) Jo, Y.-M.; Kim, D.-H.; Wang, J.; Oppenheim, J. J.; Dincă, M. Humidity-Mediated Dual Ionic−Electronic Conductivity Enables High Sensitivity in MOF Chemiresistors. *J. Am. Chem. Soc.* **2024**, *146*, 20213−20220.
(11) Lu, C.; Choi, J. Y.; Check, B.; Fang, X.; Spotts, S.; Nuñez, D.; Park, J. Thiatruxene-Based Conductive MOF: Harnessing Sulfur Chemistry for Enhanced Proton Transport. *J. Am. Chem. Soc.* **2024**, *146*, 26313−26319.
(12) Calbo, J.; Golomb, M. J.; Walsh, A. Redox-Active Metal-Organic Frameworks for Energy Conversion and Storage. *J. Mater. Chem. A* **2019**, *7*, 16571−16597.
(13) Park, S. S.; Hontz, E. R.; Sun, L.; Hendon, C. H.; Walsh, A.; Van Voorhis, T.; Dincă, M. Cation-Dependent Intrinsic Electrical Conductivity in Isostructural Tetrathiafulvalene-Based Microporous Metal-Organic Frameworks. *J. Am. Chem. Soc.* **2015**, *137*, 1774−1777.
(14) Wang, H.-Y.; Ge, J.-Y.; Hua, C.; Jiao, C.-Q.; Wu, Y.; Leong, C. F.; D'Alessandro, D. M.; Liu, T.; Zuo, J.-L. Photo- and Electronically Switchable Spin-Crossover Iron(II) Metal-Organic Frameworks Based on a Tetrathiafulvalene Ligand. *Angew. Chem., Int. Ed.* **2017**, *56*, 5465−5470.
(15) Castells-Gil, J.; Mañas-Valero, S.; Vitórica-Yrezábal, I. J.; Ananias, D.; Rocha, J.; Santiago, R.; Bromley, S. T.; Baldoví, J. J.; Coronado, E.; Souto, M.; Mínguez Espallargas, G. Electronic, Structural and Functional Versatility in Tetrathiafulvalene-Lanthanide Metal−Organic Frameworks. *Chem.—Eur. J.* **2019**, *25*, 12636−12643.
(16) Xie, L. S.; Alexandrov, E. V.; Skorupskii, G.; Proserpio, D. M.; Dincă, M. Diverse $\pi-\pi$ Stacking Motifs Modulate Electrical Conductivity in Tetrathiafulvalene-Based Metal−Organic Frameworks. *Chem. Sci.* **2019**, *10*, 8558−8565.
(17) Su, J.; Hu, T. H.; Murase, R.; Wang, H. Y.; D'Alessandro, D. M.; Kurmoo, M.; Zuo, J. L. Redox Activities of Metal-Organic Frameworks Incorporating Rare-Earth Metal Chains and Tetrathiafulvalene Linkers. *Inorg. Chem.* **2019**, *58*, 3698−3706.
(18) Zhang, S.; Panda, D. K.; Yadav, A.; Zhou, W.; Saha, S. Effects of Intervalence Charge Transfer Interaction between π-Stacked Mixed Valent Tetrathiafulvalene Ligands on the Electrical Conductivity of 3D Metal−Organic Frameworks. *Chem. Sci.* **2021**, *12*, 13379−13391.
(19) Zigon, N.; Solano, F.; Auban-Senzier, P.; Grolleau, S.; Devic, T.; Zolotarev, P. N.; Proserpio, D. M.; Barszcz, B.; Olejniczak, I.; Avarvari, N. A Redox Active Rod Coordination Polymer from Tetrakis(4-Carboxylic Acid Biphenyl)Tetrathiafulvalene. *Dalton Trans* **2024**, *53*, 4805−4813.
(20) Wang, H.-Y.; Su, J.; Zuo, J.-L. Porous Crystalline Materials Based on Tetrathiafulvalene and Its Analogues: Assembly, Charge Transfer, and Applications. *Acc. Chem. Res.* **2024**, *57*, 1851−1869.
(21) Su, J.; He, W.; Li, X.-M.; Sun, L.; Wang, H.-Y.; Lan, Y.-Q.; Ding, M.; Zuo, J.-L. High Electrical Conductivity in a 2D MOF with Intrinsic Superprotonic Conduction and Interfacial Pseudo-Capacitance. *Matter* **2020**, *2*, 711−722.
(22) Bao, S.-S.; Shimizu, G. K. H.; Zheng, L.-M. Proton Conductive Metal Phosphonate Frameworks. *Coord. Chem. Rev.* **2019**, *378*, 577−594.
(23) Zhang, Y.; Wang, J.; Apostol, P.; Rambabu, D.; Eddine Lakraychi, A.; Guo, X.; Zhang, X.; Lin, X.; Pal, S.; Rao Bakuru, V.; Chen, X.; Vlad, A. Bimetallic Anionic Organic Frameworks with Solid-State Cation Conduction for Charge Storage Applications. *Angew. Chem., Int. Ed.* **2023**, *62*, No. e202310033.
(24) Vilela, S. M. F.; Navarro, J. A. R.; Barbosa, P.; Mendes, R. F.; Pérez-Sánchez, G.; Nowell, H.; Ananias, D.; Figueiredo, F.; Gomes, J. R. B.; Tomé, J. P. C.; Paz, F. A. A. Multifunctionality in an Ion-Exchanged Porous Metal−Organic Framework. *J. Am. Chem. Soc.* **2021**, *143*, 1365−1376.
(25) Pili, S.; Argent, S. P.; Morris, C. G.; Rought, P.; García-Sakai, V.; Silverwood, I. P.; Easun, T. L.; Li, M.; Warren, M. R.; Murray, C. A.; Tang, C. C.; Yang, S.; Schröder, M. Proton Conduction in a Phosphonate-Based Metal−Organic Framework Mediated by Intrinsic "Free Diffusion inside a Sphere. *J. Am. Chem. Soc.* **2016**, *138*, 6352−6355.
(26) Taddei, M.; Shearan, S. J. I.; Donnadio, A.; Casciola, M.; Vivani, R.; Costantino, F. Investigating the Effect of Positional Isomerism on the Assembly of Zirconium Phosphonates Based on Tritopic Linkers. *Dalton Trans* **2020**, *49*, 3662−3666.
(27) Huang, Y.; Zhou, F.; Feng, J.; Zhao, H.; Qi, C.; Ji, J.; Bao, S.; Zheng, T. An Ultra-Stable Hafnium Phosphonate MOF Platform for Comparing the Proton Conductivity of Various Guest Molecules/Ions. *Chem. Commun.* **2021**, *57*, 1238−1241.

https://doi.org/10.1021/jacs.4c13792
J. Am. Chem. Soc. 2025, 147, 63−68

(28) Salcedo-Abraira, P.; Biglione, C.; Vilela, S. M. F.; Svensson Grape, E.; Ureña, N.; Salles, F.; Pérez-Prior, M. T.; Willhammar, T.; Trens, P.; Várez, A.; Inge, A. K.; Horcajada, P. High Proton Conductivity of a Bismuth Phosphonate Metal−Organic Framework with Unusual Topology. *Chem. Mater.* **2023**, *35*, 4329−4337.
(29) Siemensmeyer, K.; Peeples, C. A.; Tholen, P.; Schmitt, F.; Çoşut, B.; Hanna, G.; Yücesan, G. Phosphonate Metal−Organic Frameworks: A Novel Family of Semiconductors. *Adv. Mater.* **2020**, *32*, 2000474.
(30) Peeples, C. A.; Kober, D.; Schmitt, F.; Tholen, P.; Siemensmeyer, K.; Halldorson, Q.; Çoşut, B.; Gurlo, A.; Yazaydin, A. O.; Hanna, G.; Yücesan, G. A 3D Cu-Naphthalene-Phosphonate Metal−Organic Framework with Ultra-High Electrical Conductivity. *Adv. Funct. Mater.* **2021**, *31*, 2007294.
(31) Mitamura, Y.; Yorimitsu, H.; Oshima, K.; Osuka, A. Straightforward Access to Aryl-Substituted Tetrathiafulvalenes by Palladium-Catalysed Direct C−H Arylation and Their Photophysical and Electrochemical Properties. *Chem. Sci.* **2011**, *2*, 2017−2021.
(32) Ribeiro, C.; Valente, G.; Espinosa, M.; Silva, R. A. L.; Belo, D.; Gil-Guerrero, S.; Arisnabarreta, N.; Mali, K. S.; De Feyter, S.; Melle-Franco, M.; Souto, M. Direct C−H Arylation of Dithiophene-Tetrathiafulvalene: Tuneable Electronic Properties and 2D Self-Assembled Molecular Networks at the Solid/Liquid Interface. *Chem.—Eur. J.* **2023**, *29*, No. e202300572.
(33) Conibear, A. C.; Lobb, K. A.; Kaye, P. T. 31P NMR Kinetic Study of the Tandem Cleavage of Phosphonate Esters by Bromotrimethylsilane. *Tetrahedron* **2010**, *66*, 8446−8449.
(34) Umland, T. C.; Allie, S.; Kuhlmann, T.; Coppens, P. Relation between Geometry and Charge Transfer in Low-Dimensional Organic Salts. *J. Phys. Chem.* **1988**, *92*, 6456−6460.
(35) Souto, M.; Romero, J.; Calbo, J.; Vitorica-Yrezabal, J.; Zafra, J. L.; Casado, J.; Ortí, E.; Walsh, A.; Mínguez Espallargas, G. Breathing-Dependent Redox Activity in a Tetrathiafulvale-Based Metal-Organic Framework. *J. Am. Chem. Soc.* **2018**, *140*, 10562−10569.
(36) Pili, S.; Argent, S. P.; Morris, C. G.; Rought, P.; García-Sakai, V.; Silverwood, I. P.; Easun, T. L.; Li, M.; Warren, M. R.; Murray, C. A.; Tang, C. C.; Yang, S.; Schröder, M. Proton Conduction in a Phosphonate-Based Metal−Organic Framework Mediated by Intrinsic "Free Diffusion inside a Sphere. *J. Am. Chem. Soc.* **2016**, *138*, 6352−6355.
(37) Hadjiivanov, K. I.; Panayotov, D. A.; Mihaylov, M. Y.; Ivanova, E. Z.; Chakarova, K. K.; Andonova, S. M.; Drenchev, N. L. Power of Infrared and Raman Spectroscopies to Characterize Metal-Organic Frameworks and Investigate Their Interaction with Guest Molecules. *Chem. Rev.* **2021**, *121*, 1286−1424.
(38) Reichenau, T. M.; Steinke, F.; Wharmby, M. T.; Näther, C.; Engesser, T. A.; Stock, N. Targeted Synthesis of a Highly Stable Aluminium Phosphonate Metal−Organic Framework Showing Reversible HCl Adsorption. *Angew. Chem., Int. Ed.* **2023**, *135*, No. e202303561.
(39) Souto, M.; Santiago-Portillo, A.; Palomino, M.; Vitórica-Yrezábal, I. J.; Vieira, B. J. C.; Waerenborgh, J. C.; Valencia, S.; Navalón, S.; Rey, F.; García, H.; Mínguez Espallargas, G. A Highly Stable and Hierarchical Tetrathiafulvalene-Based Metal-Organic Framework with Improved Performance as a Solid Catalyst. *Chem. Sci.* **2018**, *9*, 2413−2418.
(40) Chen, B.; Lv, Z. P.; Leong, C. F.; Zhao, Y.; D'Alessandro, D. M.; Zuo, J. L. Crystal Structures, Gas Adsorption, and Electrochemical Properties of Electroactive Coordination Polymers Based on the Tetrathiafulvalene-Tetrabenzoate Ligand. *Cryst. Growth Des.* **2015**, *15*, 1861−1870.
(41) Valente, G.; Esteve-Rochina, M.; Paracana, A.; Rodríguez-Diéguez, A.; Choquesillo-Lazarte, D.; Ortí, E.; Calbo, J.; Ilkaeva, M.; Mafra, L.; Hernández-Rodríguez, M. A.; Rocha, J.; Alves, H.; Souto, M. Through-Space Hopping Transport in an Iodine-Doped Perylene-Based Metal−Organic Framework. *Mol. Syst. Des. Eng.* **2022**, *7*, 1065−1072.
(42) Otsubo, K.; Nagayama, S.; Kawaguchi, S.; Sugimoto, K.; Kitagawa, H. A Preinstalled Protic Cation as a Switch for Superprotonic Conduction in a Metal−Organic Framework. *JACS Au* **2022**, *2*, 109−115.
(43) Wiers, M. W.; Foo, M.-L.; Balsara, N. P.; Long, J. R. A Solid Lithium Electrolyte via Addition of Lithium Isopropoxide to a Metal−Organic Framework with Open Metal Sites. *J. Am. Chem. Soc.* **2011**, *133*, 14522−14525.

https://doi.org/10.1021/jacs.4c13792
J. Am. Chem. Soc. 2025, 147, 63−68